Aberrant hippocampal neurogenesis produces glial cells in epilepsy: new targets for regenerative medicine

Toby Segasby[1, 2], Roozbeh Sanaei[1, 2], Natalija Aleksejenko[1, 2], Omar Mamad[3, 4], David C. Henshall[3, 4], Achilleas Floudas[1, 2, 5], Janosch P. Heller[1, 2, 6, 7, *]

https://doi.org/10.4103/REGENMED.REGENMED-D-24-00008

Date of submission: August 31, 2024

Date of decision: December 7, 2024

Date of acceptance: December 13, 2024

Date of web publication: February 6, 2025

From the Contents

Graphical Abstract

Epilepsy drives adult hippocampal neurogenesis to produce more glial cells than neurons as seen in mice and humans

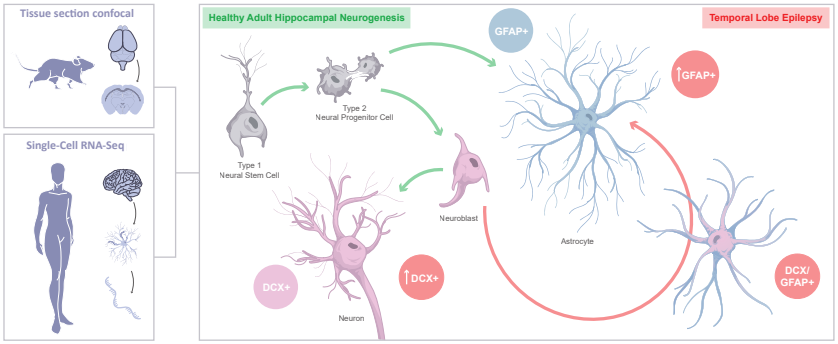

Abstract

Epilepsy is often seen to present with perturbations to adult hippocampal neurogenesis, a process intrinsically linked with neuro-regeneration and plasticity in the brain. As adult-born neurons are exceptionally rare within the nervous system, adult hippocampal neurogenesis is an attractive target for regenerative medicine. The increased neuronal activity in the epileptic brain leads to increased production of newborn cells and altered integration of new neurons within the hippocampus. Glial cells are important contributors to the neurogenic niche and astrocytes also exhibit a specific pathological response in the hippocampus of temporal lobe epilepsy patients. Here, we set out to investigate the increased number of astrocytes following status epilepticus and their association with adult hippocampal neurogenesis. Initial investigations employed immunolabeling of brain sections from the mouse intra-amygdala kainic acid model of epilepsy and were corroborated with publicly available single-cell RNA sequencing datasets of human tissue to assess newborn cells in the dentate gyrus. We found an increased number of immature neurons and reactive astrocytes in the epileptic mouse hippocampus. Additionally, we identified a cell population that expressed both neurogenesis (doublecortin) and astrocyte (glial fibrillary acidic protein) markers in the epileptic brain of both mice and humans. We further evaluated the expression profile of this cell population. Immunolabeling of mouse tissue showed that cells expressing both, doublecortin and glial fibrillary acidic protein, also expressed mature astrocyte markers aquaporin 4 and glutamate transporter-1. Human single-cell RNA sequencing data highlighted the expression of neurogenesis and astrocyte markers in the doublecortin/glial fibrillary acidic protein-expressing cells. These findings suggest chronic epilepsy may drive early neuroblasts to fate-switch to an astrocyte lineage. Further studies may reveal the mechanisms that promote neuroblast fate-switching and whether this can or should be prevented, thereby providing new targets for regenerative medicine in epilepsy and perhaps other neurologic diseases.

Key Words: adult hippocampal neurogenesis; astrocyte; biomedical engineering; doublecortin; epilepsy; glial fibrillary acidic protein; regenerative medicine; single-cell RNA sequencing

Introduction

Adult hippocampal neurogenesis (AHN) occurs within the dentate gyrus of the hippocampus. Here, neural stem cells generate immature neurons which ultimately differentiate into new granule cells.[1,2] This has been demonstrated in several animals, but the occurrence of adult neurogenesis in humans is still under debate.[1,3-5] Newborn immature neurons undergo a series of differentiation and migratory steps before integrating into existing circuits.[1,2] AHN has attracted much attention due to its role in learning and memory.[2,6] Learning and exercise have been shown to increase the number of new neurons in the dentate gyrus[7-9] and increasing neurogenesis rescues cognitive function in old age.[6]

In brain pathologies such as Alzheimer's disease, newly generated neurons within the dentate gyrus can form aberrant connections, further exacerbating the damage occurring in the brain.[10] Moreover, astrocyte changes and increased astrogliosis disrupt the regulation of neural stem cells in the dentate gyrus.[11] Additionally, problems with AHN have been described in epilepsy.[12-17] Increased neuronal activity leads to aberrant production of newborn cells, increased mossy fiber sprouting, and altered integration of new neurons within the hippocampus. These changes can drive the generation of seizures and the establishment of epilepsy.[18,19]

Doublecortin (DCX) expression has been widely used as a marker for immature neurons.[1,20] DCX is a microtubule-associated protein and is an

[1]School of Biotechnology, Dublin City University, Dublin, Ireland; [2]DCU Life Sciences Institute, Dublin City University, Dublin, Ireland; [3]Department of Physiology and Medical Physics, RCSI University of Medicine and Health Sciences, Dublin, Ireland; [4]FutureNeuro SFI Research Centre, RCSI University of Medicine and Health Sciences, Dublin, Ireland; [5]Translational Immunology Group, Medical School, University of Ioannina, Ioannina, Greece; [6]Queen Square Institute of Neurology, University College London, Queen Square, London, UK; [7]Biodesign Europe, Dublin City University, Dublin, Ireland
***Correspondence to:** Janosch P. Heller, PhD, Janosch.heller@dcu.ie.
https://orcid.org/0000-0002-8825-3787 (Janosch P. Heller)

***Funding:** This work was supported by funding from Science Foundation Ireland and FutureNeuro industry partners (16/RC/3948, 21/RC/10294_P2; to DCH); the SFI-IRC Pathway Programme (MiR-CDD, 22/PATH-S/10668; to OM); the Health Research Board (HRBEIA 2022-002; to AF); and the Irish Research Council (EpiGlymph, IRCLA/2022/3828; to JPH).*
***How to cite this article:** Segasby T, Sanaei R, Aleksejenko N, Mamad O, Henshall DC, Floudas A, Heller JP. Aberrant hippocampal neurogenesis produces glial cells in epilepsy: new targets for regenerative medicine. Regen Med Rep. 2025;2(1):7-14.*

essential protein facilitating the migration of newborn neurons.[21] However, the expression of DCX is not limited to newborn neurons. For example, its expression has been shown in astrocytes in the human neocortex.[22]

In addition to this, DCX-positive cells that resemble astrocytes morphologically and express glial fibrillary acidic protein (GFAP) have also been identified in epilepsy models.[14,16,23] A recent study has also shown that under physiological conditions, a small number of DCX-positive cells are not fully committed to neuronal differentiation and are able to regress and differentiate into astrocytes.[23] As seen in other studies, the type of chemoconvulsant used to induce epilepsy has an impact on how AHN is affected.[12,14,16,23] Although pilocarpine and kainic acid both increase the number of newborn cells, kainic acid specifically drives these cells into a glial cell fate.[12,23]

The aim of this study is to identify a novel pathway for the amelioration of AHN in epilepsy beyond neuronal production, integration, and survival. Additionally, the study also characterizes the result of AHN fate switching in human temporal lobe epilepsy (TLE).

Methods

Animals

All procedures were performed in accordance with the principles of the European Union Directive (2010/63/EU) and were reviewed and approved by the Research Ethics Committee of the Royal College of Surgeons Ireland (RCSI) (REC 1587, approval date: December 17, 2018) under license from the Health Products Regulatory Authority (AE19127/P057). This study was reported in accordance with the ARRIVE 2.0 guidelines (Animal Research: Reporting of *In Vivo* Experiments).[24] All animals were housed together on a 12-hour light-dark cycle under controlled conditions (temperature: 20–25°C; humidity: 40%–60%). Food and water were available *ad libitum* and efforts were made to minimize animal suffering and adhere to the 3R's. For the intra-amygdala kainic acid (IAKA) model of TLE and matched phosphate buffer solution (PBS) controls, 10-week-old (body weight 28–30 g) male C57BL/6OlaHsd mice originally from Harlan Laboratories (UK) and inbred at the Biomedical Research Facility at RCSI were used. Mice were positive to *Murine norovirus* and *Emtamoeba muris*. Female mice were not included in this study as the epilepsy model has historically been optimized for male mice, and the sections used here were obtained from tissue archived from a previous study.

Epilepsy models

Induction of status epilepticus using the IAKA technique was performed as previously described.[25] Briefly, mice were anesthetized (isoflurane; 5% induction, 1%–2% maintenance; Vetpharma Animal Health S.L., Barcelona, Spain) and equipped with a cannula (on the dura mater following coordinates from adjusted Bregma: IA: anterior/posterior (A/P) = −0.95 mm, lateral (L) = −2.85 mm, ventral (V) = 3.1 mm)[26] for subsequent application of kainic acid or PBS in awake animals.

Within 48 hours of cannula implantation surgery, mice randomly received either PBS (0.2 µL) or IAKA microinjection (0.3 µg KA in 0.2 µL PBS; Sigma-Aldrich, Arklow, Ireland) to induce status epilepticus (three animals received PBS and three received kainic acid). Forty minutes later, animals received an intraperitoneal (i.p.) injection of lorazepam (8 mg/kg, Pfizer, Dublin, Ireland) to ease convulsions and reduce mortality. Mice were allowed to recover in an incubator at 26°C.

Two weeks after IAKA or PBS injection, mice were sacrificed and perfused transcardially with 4% paraformaldehyde. Brains were dissected and placed in 4% PFA overnight at 4°C, and then stored in PBS supplemented with 0.01% sodium azide at 4°C until sectioning.

Immunohistochemistry

For sectioning, brains were embedded in 2% agarose and fixed to the vibratome submerged in 200 mM glycine in PBS. Sections were made coronally at 30 µm intervals from posterior to anterior and stored in PBS supplemented with 0.01% sodium azide at 4°C until staining.

Sections from three IAKA and three PBS animals were placed into wells in staining pairs free floating. The tissue was first washed with PBS before quenching with 10 mM $CuSO_4$ in 50 mM NH_4Cl for 10 minutes. Sections then underwent successive wash steps, first in ddH_2O, then PBS before blocking in 3% BSA in 0.3% PBS + t (PBS 0.3% Triton X-100) for 3 hours at room temperature. The sections were then incubated in 1% BSA in 0.1% PBS + t with primary antibodies rabbit anti-DCX (1:250, Thermo Fisher Scientific, Waltham, MA, USA, Cat# 481200, RRID: AB_2533840), mouse anti-GFAP (1:1000, Thermo Fisher Scientific, Cat# 14-9892-82, RRID: AB_10598206), and guinea pig anti-aquaporin 4 (AQP4; 1:250, Synaptic Systems, Goettingen, Germany, Cat# 429004, RRID: AB_2802156) or guinea pig anti-glutamate transporter 1 (GLT-1; 1:1000, Merck KGaA, Darmstadt, Germany, Cat# AB1783, RRID: AB_90949) overnight at 4°C. The following day, tissue sections were washed in PBS and 0.1% PBS + t before incubating in secondary antibodies goat anti-guinea pig Alexa Fluor 488 (1:500, Thermo Fisher Scientific, Cat# A11073, RRID: AB_2534117), donkey anti-rabbit Alexa Fluor 594 (1:500, Thermo Fisher Scientific, Cat# A21207, RRID: AB_141637), goat anti-mouse CF680 (1:500, Merck KGaA, Cat# SAB4600361, RRID: AB_3492091) and the nuclei stain Hoechst 33342 (1:10,000, Merck KGaA, Cat# 14533) in 1% BSA in 0.1% PBS + t at room temperature for 3 hours in the dark. Following further successive washing in 0.1% PBS + t, sections were mounted on glass slides with ProLong Diamond Antifade Mountant (Thermo Fisher Scientific, Cat# P36961).

Image acquisition

Images were acquired on a Leica Stellaris laser scanning confocal with Power HyD S detectors (Leica Microsystems, Wetzlar, Germany), running Las X. Tile scans were performed with a 20× air objective for each hemisphere, maintaining zoom factor, laser intensities, and Z thickness with 37 1 µm step increments in 1024 × 1024 format. Channels were imaged sequentially in z. Tiles had a 10% overlap and were statistically blended in the Las X software. Qualitative single frame images were acquired instead with a 100× oil objective with 37 step increments of 0.75 µm in 1024 × 1024 format. The full acquisition settings are shown in **Table 1.**

All image analysis was performed using ImageJ version 1.54 by Fiji[27] (https://imagej.net/software/fiji/). For fluorescence Intensity, regions of interest (ROIs) were created for each layer of the dentate gyrus (molecular layer, granule cell layer, and hilus; **Figure 1A**) using the Hoechst channel, with molecular layer boundaries confirmed with either AQP4 or GLT-1. ROIs were then applied to SUM slices Z-projections of each channel stack for mean grey value measurements. Cell counts were performed manually with Fiji cell counter for DCX expression and counter labels. Only cells with discernible cell body staining were counted.

Single-cell RNA sequencing datasets

We performed secondary data analysis of single-cell RNA sequencing (scRNA-seq) datasets - GSE140393[28] (https://www.ncbi.nlm.nih.gov/geo/query/acc.cgi?acc=GSE140393) and GSE209552[29] (https://www.ncbi.nlm.nih.gov/geo/query/acc.cgi?acc=GSE209552). We used the scRNA-seq data from five human epileptic patients with medically refractory TLE (GSE140393 dataset) and three temporal lobe tissue samples from non-neurological decedents as healthy controls (GSE209552 dataset).

Single-cell RNA sequencing clustering and gene expression analysis

Using the Seurat package[30] (v. 5.1.0, https://satijalab.org/seurat/) in R (v. 4.1, https://www.R-project.org/), single cell reads from each sample were converted into Seurat objects, with data filtered so that genes detected in fewer than three cells for each object were excluded from downstream analyses. Cell doublets were identified and removed in each object using Doubletfinder[31] (code available here: https://github.com/chris-mcginnis-ucsf/DoubletFinder). The SCTransform[32,33] (v. 0.4.1) workflow was used to normalize and scale the data (code available here: https://satijalab.org/seurat/reference/sctransform); to normalize for differences in sequencing depth and stabilize gene-specific variances, sctransform removes unwanted variation by incorporating additional covariates and applies a log transformation to the data, resulting in an expression matrix suitable for downstream clustering and differential expression analysis. For clustering, individual objects were merged, normalized, and scaled. Principle component analysis (PCA) was applied to the merged object to identify variable genes as input for clustering. Prior to clustering, a recently introduced function called IntegrateLayers (method=RPCAIntegration) was used to perform integration, which helps to co-embed common cell types and states across datasets using the cell's PCA coordinates (code available here: https://satijalab.org/seurat/articles/seurat5_integration). Seurat's FindNeighbors and FindClusters functions were used to identify the clusters, which were then visualized using a UMAP plot. Basic annotation was performed using key known markers of resident cells in the temporal lobe. Plotting the co-expression of GFAP and DCX markers of interest led us to target a cluster for further analysis. By subsetting this cluster, normalization, scaling, and PCA were performed followed by integration and clustering. We used the integration method harmony due to low cell numbers in cluster 11.

Table 1 | **Acquisition settings for quantification of confocal imaging**

System	Single frame Z stack	Tile Z stack
Format	1024 × 1024	1024 × 1024
Speed	400	600
Zoom factor	1	2
Image size	116.82 µm ×116.82 µm	58.12 µm × 58.12 µm
Pixel size	114.19 nm × 114.19 nm	56.82 nm × 56.82 nm
Optical section	0.895µm	2.055 µm
Pixel dwell time	1.58µs	862 ns
Frame rate	0.063/s	0.121/s
Line average	1	1
Frame average	2	1
Airy unit	1	1
Pinhole	1	1
Number of steps	37	37
Z-Step size	0.750 µm	1 µm
Tile overlap	–n/a	10%
Tile blend	n/a	Statistical

Probe			100× objective		20× objective	
Primary	Secondary	Excitation wavelength (nm)	laser power	Detector window	laser power	Detector window
Ms-GFAP	CF680	681	10	690–823	10	690–823
Rb-DCX	AF594	590	30	597–650	30	597–650
Gp-AQP4	AF488	499	10	504–601	10	504–601
Gp-GLT-1	AF488	499	15	504–601	15	504–601
–	Hoechst 33342	405	2	425–500	2	425–500

All imaged, TauMode: Intensity, Operating mode: Analog, Gain 2.50---. AQP4: Aquaporin-4; DCX: doublecortin; GFAP: glial fibrillary acidic protein; GLT-1: glutamate transporter 1.

Statistical analysis

All data comparisons between disease (KA) and control (PBS) groups across the layers of the dentate gyrus, and of the dentate gyrus as a whole, were performed using one-way analysis of variance with Tukey's *post hoc* test. A *P*-value less than 0.05 was deemed statistically significant. The confidence interval was 95%. GraphPad Prism software (GraphPad Software Inc., Domatics, CA, USA, version Prism 10.3.0) was used to perform all statistical analyses.

Results

Confirmation of model effects

Aberrant AHN has previously been described in epilepsy,[13,15,17,19] including in the IAKA mouse model used presently.[15] The findings of most studies are based on Bromodeoxyuridine (BrdU) incorporation in dividing cells as well as the expression of DCX. Peculiarly, the expression of the immature neuronal marker DCX has been shown in other cell types, including astrocytes.[22] Aberrant proliferation and location of DCX-positive cells have been reported in rodent models of epilepsy, with the presence of DCX- and GFAP-positive cells also characterized.[14,16,23]

First, we assessed GFAP expression in tissue from the IAKA model (**Figure 1**). In agreement with previous studies,[34-36] we saw an increase in GFAP expression highlighting astrogliosis and the presence of reactive astrocytes in the epileptic tissue (**Figure 1**). We found an increase in GFAP in the contralateral as well as ipsilateral dentate gyrus in the IAKA model. GFAP-positive cells in the model featured thicker processes with less branches, highlighting the hypertrophy of reactive astrocytes.

To get a better understanding of the regions within the dentate gyrus that showed the highest upregulation of GFAP, we performed analysis of fluorescence intensities in the molecular layer, the granule cell layer and the hilus subregions (highlighted as dashed white line in **Figure 1A**). The molecular layer displayed the largest increase in GFAP immunoreactivity, followed by the granule cell layer (**Figure 1C**). No significant difference in GFAP presence was found in the hilus (**Figure 1C**).

Next, we visualized the presence of DCX throughout the dentate gyrus. DCX-positive cells were scattered throughout the subgranular zone with DCX-positive processes extending through the granule cell layer (**Figure 1**). When comparing fluorescence intensities across the different layers of the dentate gyrus, we did not see a difference between PBS and IAKA at 2 weeks following status epilepticus (SE) in either hemisphere (**Figure 1C**). However, when counting DCX-positive cells, there was an increase in the number of cells in our model in the ipsilateral and the contralateral dentate gyrus compared to the PBS-injected brains (**Figure 1D**). Interestingly, when performing co-labeling of GFAP and DCX, we were able to identify a population of DCX-/GFAP-positive cells in the subgranular zone (**Figure 1D**). DCX-positive cells were morphologically generally neuronal, with polarized processes from the lower granule cell layer out to the molecular layer. In KA tissue, however there were visually denser neuronal processes with discrete unpolarized DCX signal in GFAP-positive cells (**Figure 1A** and **B**). Importantly, the number of double-positive cells was markedly increased in the IAKA model (33% ± 10% in the ipsilateral dentate gyrus), with even a small number of DCX-/GFAP-positive cells present in the contralateral dentate gyrus (**Figure 1D**). We were not able to find any double-positive cells in the PBS-injected animals. As such, consistent with expectations of the IAKA model at 2 weeks we demonstrate an increase in GFAP intensity and emergence of a DCX-/GFAP-positive cell population.

Presence of doublecortin/glial fibrillary acidic protein-positive cells in human epilepsy

To validate the mouse model finding and assess whether these cells are also present in human epilepsy, we took advantage of publicly available scRNA-Seq data. We used two data sets of the human temporal lobe, one control [GSE209552][29] and one epilepsy [GSE140393][28] datasets. First, samples underwent pre-filtering followed by normalization, scaling, and integration to minimize the effects of technical sources of variation. Clustering resulted in 20 clusters in the control tissue (**Figure 2A**). None of the clusters were positive for *DCX* and *GFAP* together. Clustering of the epilepsy data set resulted in 16 distinct cell clusters (**Figure 2B**). One of these clusters (cluster 11) showed co-expression of *GFAP* and *DCX* (**Figure 2B**). The feature plots of the individual clusters revealed that cells of cluster 11 expressed glial cell markers *EAAT2* (excitatory amino acid transporter 2, *GLT-1*, *SLC1A2*), *OLIG2* (oligodendrocyte transcription factor 2) (**Figure 2C**), neurogenesis markers *GFAP*, *DCX*, *SOX2* (SRY (sex determining region Y)-box 2), *ASCL1* (achaete-scute homolog 1), *NCAM1* (neural cell adhesion molecule 1) (**Figure 2B** and **D**), astrocyte markers *S100beta*, *EAAT1* (*GLAST*, *SLC1A3*) (**Figure 2E**), NG2 cell markers *CSPG4* (chondroitin sulfate proteoglycan 4) and *BEX1* (brain-expressed X-linked protein 1) (**Figure 2F**), and neuronal markers *MAP2* (microtubule-associated protein 2) and *THY1* (**Figure 2I**). Cluster 11 was mostly devoid of cells expressing typical markers of microglial cells (**Figure 2G**), endothelial cells (**Figure 2H**), and immune cells (**Figure 2J**). However, we also note the

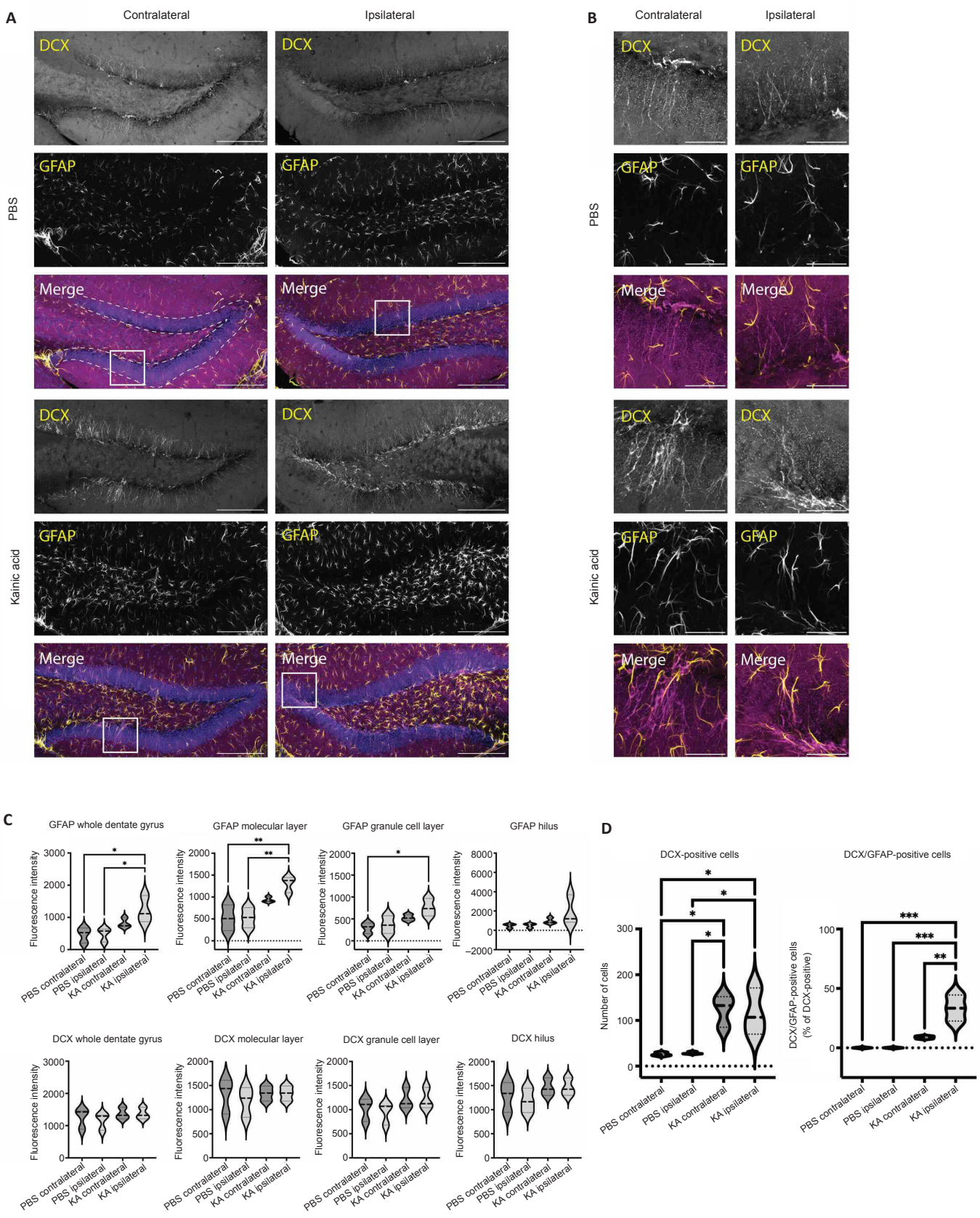

Figure 1 | **Expression of DCX and GFAP in the dentate gyrus in the IAKA model of epilepsy.**
(A) Confocal images of PBS or KA-injected brains 2 weeks post-SE. Sections were labeled with nuclei marker Hoechst (blue), GFAP (yellow), and DCX (magenta). The molecular layer, granular cell layer, and hilus subregions are highlighted with white dashed lines. (B) Area shown by white square in A at higher magnification. Scale bars: 200 µm (A) and 50 µm (B). (C) Fluorescence intensity measurements of GFAP (top row) and DCX (bottom row) in PBS or KA-injected brain sections. (D) Cell counts of DCX-positive cells and cells positive for DCX and GFAP expressed as a percentage of DCX-positive cells. *P < 0.05, **P < 0.01, ***P < 0.001 (one-way analysis of variance with Tukey's *post hoc* test). DCX: Doublecortin; GFAP: glial fibrillary acidic protein; IAKA: intra-amygdala kainic acid; KA: kainic acid; PBS: phosphate buffered solution; SE: status epilepticus.

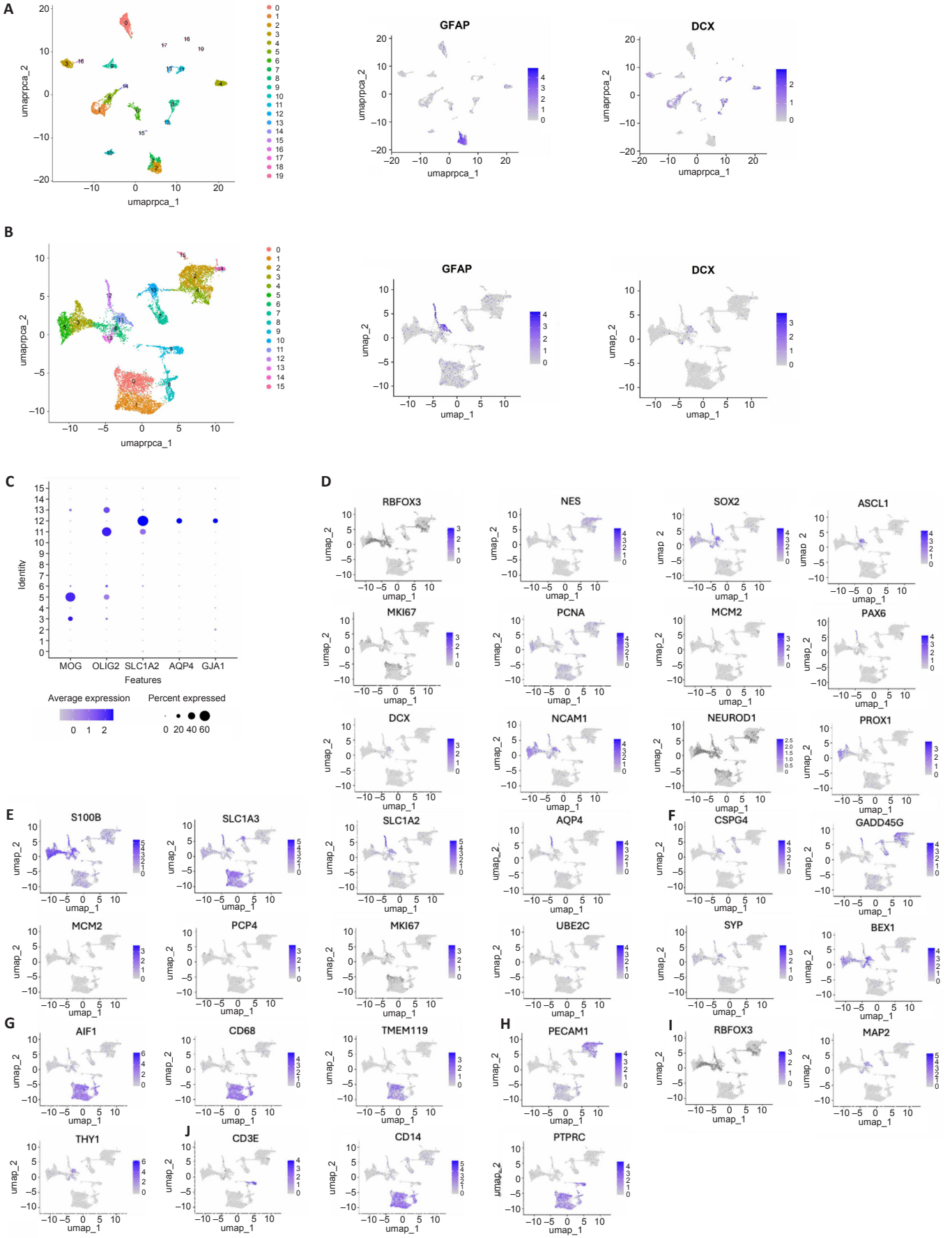

Figure 2 | **ScRNAseq data reveals an increased number of DCX/GFAP-positive cells in human epileptic temporal lobe.**
(A) UMAP plot of 20 clusters identified in the control temporal lobe tissue (left) and feature plots of GFAP and DCX expression (right). (B) UMAP plot of 16 clusters identified in the epileptic temporal lobe tissue (left) and feature plots of GFAP and DCX expression (right). (C) Plot highlighting glial cell marker expression across the 16 clusters identified in the epileptic temporal lobe tissue. (D–J) Feature plots highlighting neurogenesis (D), astrocyte (E), NG2 cell (F), microglia (G), endothelial cell (H), neuronal (I), and immune cell (J) marker expression across the 16 clusters identified in the epileptic temporal lobe tissue. DCX: Doublecortin; GFAP: glial fibrillary acidic protein.

presence of a *CD45*-positive cell infiltrate consisting primarily of *CD14*-positive monocytes/macrophages and a small population of *CD3*-positive T-cells (**Figure 2J**). Overall, cells in cluster 11 show expression features of reactive astrocytes. Distinct from the DCX-/GFAP-positive cell cluster, cluster 12 may represent mature astrocytes that have not arisen from aberrant neurogenesis expressing genes encoding important astrocyte proteins such as AQP4, S100beta, EAAT1 (GLAST, SLC1A3) and EAAT2 (GLT-1, SLC1A2) and GFAP (**Figure 2**). Therefore, we see the IAKA model findings are consistent with human epilepsy data, with the presence of a unique aberrant neurogenic-astrocyte cell cluster.

Verification of astrocyte lineage

Lastly, we wanted to explore whether the DCX-/GFAP-positive cells were functional astrocytes. As an approach, we co-labeled brain sections with DCX, GFAP, and markers of mature astrocytes, AQP4, and EAAT2/GLT-1 (**Figure 3A**). Both proteins are essential for the proper function of mature astrocytes in the healthy brain. AQP4 is the major water channel located mainly in the astrocytic endfeet which ensheath blood vessels throughout the central nervous system and plays a crucial role in brain waste clearance.[37] EAAT2/GLT-1 is the major glutamate transporter in the hippocampus, located mainly in perisynaptic astrocytic processes regulating extracellular glutamate concentrations locally at synapses.[38] The DCX-/GFAP-positive cells in the subgranular zone of the ipsilateral KA dentate gyrus express AQP4 and EAAT2/GLT-1 (**Figure 3A**).

Additionally, we performed more in-depth expression analysis of the cells identified in cluster 11. The cells of cluster 11 were further subsetted ("isolated"), re-normalized, re-scaled, and re-integrated to perform a higher resolution clustering to identify potential cellular subsets within cluster 11. Following this process, four distinct subsets of cells were identified within this cluster (**Figure 3B**). Most DCX/GFAP-positive cells were found in subcluster 3 (**Figure 3C**). As highlighted in the global expression plots in **Figure 2**, cells in cluster 11 expressed neurogenesis markers, astrocyte markers, NG2 cell markers, and neuronal markers but did not express typical markers of microglial, endothelial, and immune cells (**Figure 3D–J**).

Discussion

AHN is routinely altered under neuropathological conditions and extensively demonstrated to be changed in TLE.[13,17,19] While the main output of AHN is neuronal, there are core glial contributions at all stages.[1,2] In particular astrocytes are intimately involved in AHN and undergo extensive change across all neurological disorders including epilepsy.[34,39] Given the pathological shifts that occur in tandem between astrocytes and hippocampal neurogenesis this study sought to investigate their potential crossover.

The present study demonstrates there is increased GFAP expression in epileptic tissue in the IAKA model, corroborating previous results exploring the effects of KA administration on astrogliosis in animal models.[34-36] Astrogliogenesis is a common feature of the neuropathology of human epilepsy, including astrocytic hypertrophy, functional dysregulation, disruption to regulatory gene expression, and increased proliferation.[34-36] Moreover, in mice, inducing astrogliosis is sufficient to promote epilepsy due to alterations in neurotransmitter uptake and breakdown of adenosine, among many other mechanisms.[40,41]

We found a change in DCX expression in the KA model of TLE highlighting an arrest of physiologically healthy AHN. Interestingly, DCX intensity measurements were comparable within each layer of the dentate gyrus across all experimental hemispheres in PBS and KA tissue slices. Of note however, was the drastic change in DCX staining profile. As described above, cells expressing DCX under confocal imaging in PBS and KA hemispheres are morphologically generally neuronal. However, in KA tissue GFAP-positive cells have visually denser neuronal processes with unpolarized DCX signal. Further counter stains also demonstrate the KA ipsilateral dentate gyrus DCX/GFAP-positive signal is colocalized with mature astrocyte markers AQP4 and EAAT2/GLT-1. This staining profile was confirmed by cell counts which revealed co-expressing DCX and GFAP cells unique to epilepsy tissue. Previous work by Moura et al.[23] eloquently showed this phenomenon and it is promising to see the result conserved with more readily available methodologies in a different model.

The detection of a unique DCX/GFAP-positive population in human epilepsy is particularly exciting, providing this new perspective for regenerative medicine with meaningful translational value. Previous studies have demonstrated DCX expression in non-neuronal cells in human tissue[20] but have not previously detailed DCX/GFAP-positive cells to the extent we have been able to with scRNAseq data**.** Demonstrating DCX clustering with astrocyte-specific markers, distinct from other mature astrocyte populations proposes a new target for therapies that seek to ameliorate AHN in disease. While the presence of AQP4 was highlighted in our confirmatory imaging, future studies are needed to fully characterize this subpopulation and should show consideration for the species differences in astrocytes seen between rodents and humans.[42] Nevertheless, seeing a feature of aberrant AHN conserved from the rodent model to patient data is very promising. Future work should seek to understand if the DCX/GFAP-positive cells can be ameliorated or upregulated in disease settings. Reduced neuronal DCX is correlated with cell loss, reduced proliferation of hippocampal neural progenitor cells; or deviated differentiation in neuroblasts. Here, we demonstrate that 33% ± 10% of the elevated DCX cell counts in the ipsilateral dentate gyrus in the IAKA model were also GFAP positive. We also demonstrate an increase in GFAP intensity measurements in the granule cell layer, which together illustrate the reduction of neuronal output and favoring of astrogliosis, which is a distinct phenotype of TLE previously described.[43]

An important implication of the present findings is that the environment into which new cells are born may shift molecular features toward astrocyte rather than neuronal phenotype. While DCX is indicative of the differentiation stage and lineage, the transition from progenitor cell to final cell fate can be modified,[44] with definitive determination not allocated until later stages. Astrocytes are a physiologically healthy differentiation endpoint in AHN[45] all be it at much lower numbers than granule neurons. As astrogliosis is a fundament of TLE pathology,[34-36] and the neurogenic niche is sensitive to environmental changes, it could be possible that early neuroblasts are fate-switching to an astrocyte lineage in response to the KA insult and frequent seizures as previously hypothesized.[23] We see a stark increase in DCX-positive cells in TLE hemispheres, perhaps indicating that switching to an astroglial fate is a protective mechanism against the activity of immature cells within the circuit. Conversely, astrogliosis is a common feature of TLE with hippocampal sclerosis, and the competing signaling of cell production for both neurons and astrocytes gives rise to something in between.

GFAP is not an exclusive marker to astrocytes, however, with radial glial neural stem cells in the dentate gyrus also expressing GFAP.[46] While fate-switching of neuroblasts is a corroborated pathway for explaining DCX/GFAP-positivity, alternative research demonstrates neural progenitor cells differentiate into astrocytes following quiescence in healthy aging.[47] This could represent another route by which TLE disturbs AHN processes and achieves greater GFAP levels throughout the subgranular zone. It is also crucial to be aware that GFAP expression patterns and neural stem cell proliferation, differentiation, and survival are altered differently depending on chemoconvulsant administered.[12,14,16,23] The presence of GFAP and DCX-expressing cells in human single-cell RNA-seq is particularly important here in defining the relevance of this potential stolen fate for human disease.

Limitations

It is also prudent to highlight the limitations of this study so that future work may better address the aims of this work. The present results analyzed tissue sections and single-cell data from a relatively small number of individuals. The imaging data from the rodent model should be explored using larger animal numbers than was possible here. There was also inter-individual variability in pathology in the mouse model. With greater animal numbers, investigations may ascertain a threshold at which DCX-positive cells are predominantly neuronal or glial and be in a stronger position to ascertain what promotes the production of DCX/GFAP-positive cells. As suggested above, we demonstrate an incongruence between rodent and human expression of AQP4 in DCX/GFAP-positive cells. Future work should seek to quantifiably address this and to determine whether these are indeed the same types of cells formed in the altered neurogenesis and whether these cells should be targeted therapeutically.

Conclusions

Here, we demonstrate astrogliosis and an apparent fate-switch of early neuroblasts to an astrocyte lineage following seizures induced by IAKA injection in mice. Additionally, we confirmed the presence of DCX/GFAP-positive cells in human epileptic tissue using scRNAseq data. These cells expressed glial cell markers distinct from other astrocyte clusters. Future investigation is needed to fully characterize the DCX/GFAP-positive cells in experimental and human epilepsy and whether the aberrant production of glial cells should be treated or enhanced as a therapy in epilepsy.

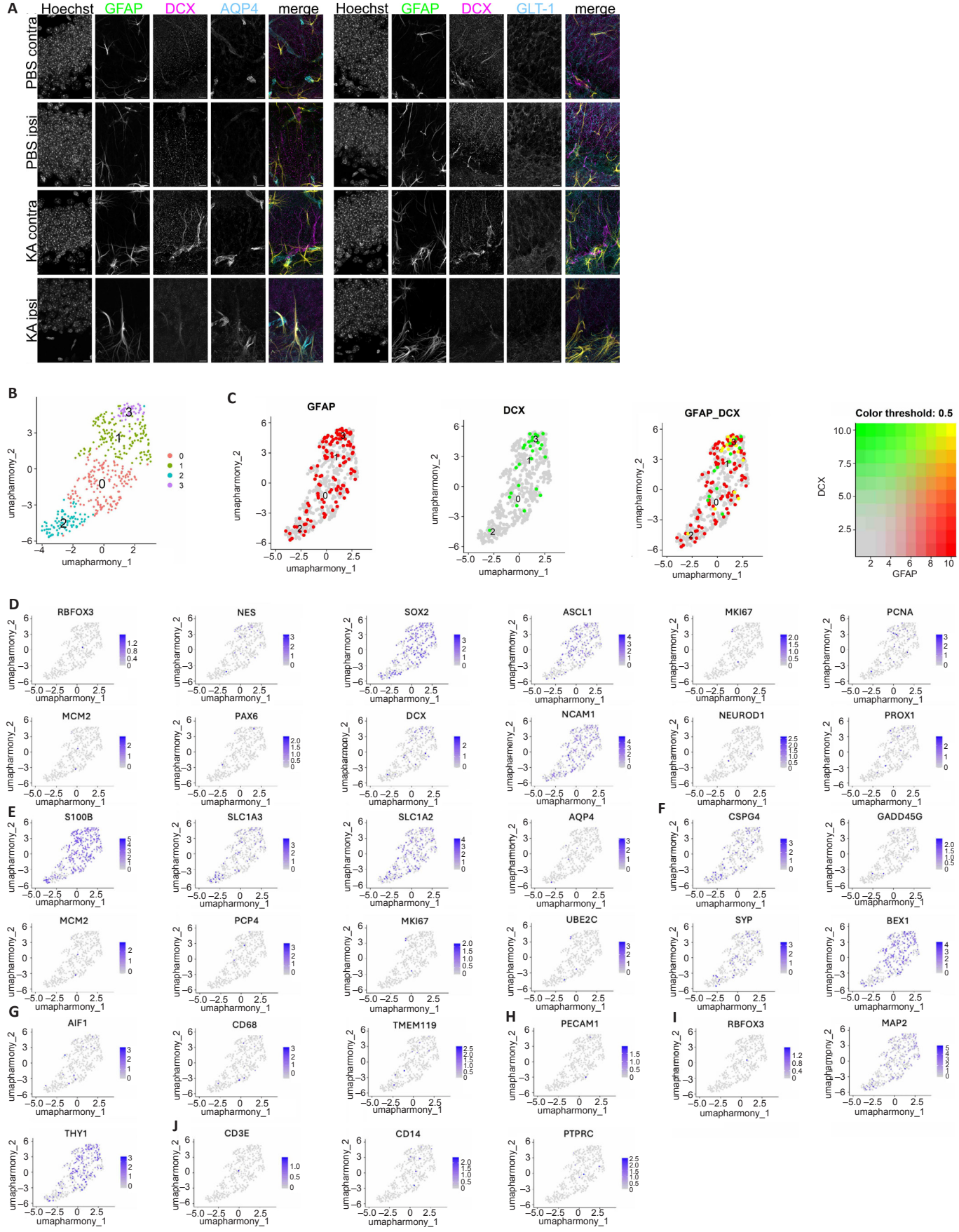

Figure 3 | **DCX/GFAP-positive cells express astrocyte markers.**

(A) Confocal images of PBS or KA-injected brains 2 weeks post-status epilepticus. Sections were labeled with Hoechst, GFAP (green), DCX (magenta) and AQP4 (cyan, left) or EAAT2/GLT-1 (cyan, right). Scale bars: 10 µm. (B) UMAP plot highlighting the four subclusters of cluster 11 in the epileptic temporal lobe tissue. (C) Feature plot highlighting GFAP and DCX expression across the four subclusters of cluster 11 in the epileptic temporal lobe tissue. (D–J) Feature plots highlighting neurogenesis (D), astrocyte (E), NG2 cell (F), microglia (G), endothelial cell (H), neuronal (I), immune cell (J) marker expression across cluster 11 in the epileptic temporal lobe tissue. AQP4: Aquaporin-4; DCX: doublecortin; EAAT2: excitatory amino acid transporter 2; GFAP: glial fibrillary acidic protein; GLT-1: glutamate transporter 1; KA: kainic acid; PBS: phosphate buffer solution.

Acknowledgments: *We thank Ms Oluwafadekemi Bello for performing preliminary experiments. Images were acquired in the RCSI Super Resolution Imaging Facility funded by Science Foundation Ireland (18/RI/5723).*

Author contributions: *Material preparation, data collection, and analysis were performed by TS, RS, NA, and OM. The first draft of the manuscript was written by TS, NA, and JPH. All authors commented on previous versions of the manuscript, contributed to the study's conception and design, and approved the final manuscript.*

Conflicts of interest: *The authors declare no conflicts of interest.*

Ethics committee approval: *All procedures were approved by the Research Ethics Committee of the Royal College of Surgeons Ireland (RCSI) (REC 1587, approval date: December 17, 2018).*

Patient consent: *Not applicable.*

Data availability statement: *All relevant data are within the paper.*

References

1. Simard S, Matosin N, Mechawar N. Adult hippocampal neurogenesis in the human brain: updates, challenges, and perspectives. *Neuroscientist*. 2024:10738584241252581. doi: 10.1177/10738584241252581
2. Kempermann G, Song H, Gage FH. Neurogenesis in the adult hippocampus. *Cold Spring Harb Perspect Biol*. 2015;7(9):a018812. doi: 10.1101/cshperspect.a018812
3. Boldrini M, Fulmore CA, Tartt AN, et al. Human hippocampal neurogenesis persists throughout aging. *Cell Stem Cell*. 2018;22(4):589-599.e5. doi: 10.1016/j.stem.2018.03.015
4. Sorrells SF, Paredes MF, Cebrian-Silla A, et al. Human hippocampal neurogenesis drops sharply in children to undetectable levels in adults. *Nature*. 2018;555(7696):377-381. doi: 10.1038/nature25975
5. Leal-Galicia P, Chávez-Hernández ME, Mata F, et al. Adult neurogenesis: a story ranging from controversial new neurogenic areas and human adult neurogenesis to molecular regulation. *Int J Mol Sci*. 2021;22(21):11489. doi: 10.3390/ijms222111489
6. Berdugo-Vega G, Arias-Gil G, López-Fernández A, et al. Increasing neurogenesis refines hippocampal activity rejuvenating navigational learning strategies and contextual memory throughout life. *Nat Commun*. 2020;11(1):135. doi: 10.1038/s41467-019-14026-z
7. Vivar C, Potter MC, Van Praag H. All about running: synaptic plasticity, growth factors and adult hippocampal neurogenesis. In: Belzung C, Wigmore P, eds. *Neurogenesis and Neural Plasticity*. *Vol 15*. *Current Topics in Behavioral Neurosciences*. Springer Berlin Heidelberg; 2012:189-210.
8. Liu PZ, Nusslock R. Exercise-mediated neurogenesis in the hippocampus via BDNF. *Front Neurosci*. 2018;12:52. doi: 10.3389/fnins.2018.00052
9. Kempermann G, Kuhn HG, Gage FH. More hippocampal neurons in adult mice living in an enriched environment. *Nature*. 1997;386(6624):493-495. doi: 10.1038/386493a0
10. Salta E, Lazarov O, Fitzsimons CP, Tanzi R, Lucassen PJ, Choi SH. Adult hippocampal neurogenesis in Alzheimer's disease: A roadmap to clinical relevance. *Cell Stem Cell*. 2023;30(2):120-136. doi: 10.1016/j.stem. 2023.01.002
11. Suárez J, de Ceglia M, Rodríguez-Pozo M, et al. Inhibition of adult neurogenesis in male mice after repeated exposure to paracetamol overdose. *Int J Mol Sci*. 2024;25(4):1964. doi: 10.3390/ijms25041964
12. Sierra A, Martín-Suárez S, Valcárcel-Martín R, et al. Neuronal hyperactivity accelerates depletion of neural stem cells and impairs hippocampal neurogenesis. *Cell Stem Cell*. 2015;16(5):488-503. doi: 10.1016/j.stem. 2015.04.003
13. Chen P, Chen F, Wu Y, Zhou B. New insights into the role of aberrant hippocampal neurogenesis in epilepsy. *Front Neurol*. 2021;12:727065. doi: 10.3389/fneur.2021.727065
14. Muro-García T, Martín-Suárez S, Espinosa N, et al. Reactive disruption of the hippocampal neurogenic niche after induction of seizures by injection of kainic acid in the amygdala. *Front Cell Dev Biol*. 2019;7:158. doi: 10.3389/fcell.2019.00158
15. Beamer EH, Jurado-Arjona J, Jimenez-Mateos EM, et al. MicroRNA-22 controls aberrant neurogenesis and changes in neuronal morphology after status epilepticus. *Front Mol Neurosci*. 2018;11:442. doi: 10.3389/fnmol.2018.00442
16. Moura DMS, de Sales IRP, Brandão JA, Costa MR, Queiroz CM. Disentangling chemical and electrical effects of status epilepticus-induced dentate gyrus abnormalities. *Epilepsy Behav*. 2021;121(Pt B):106575. doi: 10.1016/j.yebeh.2019.106575
17. Liu YWJ, Curtis MA, Gibbons HM, et al. Doublecortin expression in the normal and epileptic adult human brain. *Eur J Neurosci*. 2008;28(11):2254-2265. doi: 10.1111/j.1460-9568.2008.06518.x
18. Hosford BE, Liska JP, Danzer SC. Ablation of newly generated hippocampal granule cells has disease-modifying effects in epilepsy. *J Neurosci*. 2016;36(43):11013-11023. doi: 10.1523/JNEUROSCI.1371-16.2016
19. Cho KO, Lybrand ZR, Ito N, et al. Aberrant hippocampal neurogenesis contributes to epilepsy and associated cognitive decline. *Nat Commun*. 2015;6(1):6606. doi: 10.1038/ncomms7606
20. Liu JYW, Matarin M, Reeves C, et al. Doublecortin-expressing cell types in temporal lobe epilepsy. *Acta Neuropathol Commun*. 2018;6(1):60. doi: 10.1186/s40478-018-0566-5
21. Francis F, Koulakoff A, Boucher D, et al. Doublecortin is a developmentally regulated, microtubule-associated protein expressed in migrating and differentiating neurons. *Neuron*. 1999;23(2):247-256. doi: 10.1016/S0896-6273(00)80777-1
22. Verwer RWH, Sluiter AA, Balesar RA, et al. Mature astrocytes in the adult human neocortex express the early neuronal marker doublecortin. *Brain J Neurol*. 2007;130(Pt 12):3321-3335. doi: 10.1093/brain/awm264
23. Moura DMS, Brandão JA, Lentini C, Heinrich C, Queiroz CM, Costa MR. Evidence of progenitor cell lineage rerouting in the adult mouse hippocampus after status epilepticus. *Front Neurosci*. 2020;14:571315. doi: 10.3389/fnins. 2020.571315
24. Percie du Sert N, Hurst V, Ahluwalia A, et al. The ARRIVE guidelines 2.0: Updated guidelines for reporting animal research. *Br J Pharmacol*. 2020;177(16):3617-3624. doi: 10.1111/bph.15193.
25. Mamad O, Heiland M, Lindner AU, et al. Anti-seizure effects of JNJ-54175446 in the intra-amygdala kainic acid model of drug-resistant temporal lobe epilepsy in mice. *Front Pharmacol*. 2024;14:1308478. doi: 10.3389/fphar. 2023.1308478
26. Paxinos G, Franklin KBJ. *Paxinos and Franklin's the Mouse Brain in Stereotaxic Coordinates*. 4th ed. Boston: Elsevier/Academic Press; 2013.
27. Schindelin J, Arganda-Carreras I, Frise E, et al. Fiji: an open-source platform for biological-image analysis. *Nat Methods*. 2012;9(7):676-682. doi: 10.1038/nmeth.2019
28. Pai B, Tome-Garcia J, Cheng WS, et al. High-resolution transcriptomics informs glial pathology in human temporal lobe epilepsy. *Acta Neuropathol Commun*. 2022;10(1):149. doi: 10.1186/s40478-022-01453-1
29. Garza R, Sharma Y, Atacho D, et al. Single-cell transcriptomics of resected human traumatic brain injury tissues reveals acute activation of endogenous retroviruses in oligodendroglia. bioRxiv [Preprint]. 2022. doi: 10.1101/2022.09.07.506982
30. Hao Y, Stuart T, Kowalski MH, et al. Dictionary learning for integrative, multimodal and scalable single-cell analysis. *Nat Biotechnol*. 2024;42(2):293-304. doi: 10.1038/s41587-023-01767-y
31. McGinnis CS, Murrow LM, Gartner ZJ. DoubletFinder: doublet detection in single-cell RNA sequencing data using artificial nearest neighbors. *Cell Syst*. 2019;8(4):329-337.e4. doi: 10.1016/j.cels.2019.03.003
32. Hafemeister C, Satija R. Normalization and variance stabilization of single-cell RNA-seq data using regularized negative binomial regression. *Genome Biol*. 2019;20(1):296. doi: 10.1186/s13059-019-1874-1
33. Choudhary S, Satija R. Comparison and evaluation of statistical error models for scRNA-seq. *Genome Biol*. 2022;23(1):27. doi: 10.1186/s13059-021-02584-9
34. Vezzani A, Ravizza T, Bedner P, Aronica E, Steinhäuser C, Boison D. Astrocytes in the initiation and progression of epilepsy. *Nat Rev Neurol*. 2022;18(12):707-722. doi: 10.1038/s41582-022-00727-5
35. Twible C, Abdo R, Zhang Q. Astrocyte role in temporal lobe epilepsy and development of mossy fiber sprouting. *Front Cell Neurosci*. 2021;15:725693. doi: 10.3389/fncel.2021.725693
36. Sitovskaya D, Zabrodskaya Y, Parshakov P, et al. Expression of cytoskeletal proteins (GFAP, Vimentin), proapoptotic protein (Caspase-3) and protective protein (S100) in the epileptic focus in adults and children with drug-resistant temporal lobe epilepsy associated with focal cortical dysplasia. *Int J Mol Sci*. 2023;24(19):14490. doi: 10.3390/ijms241914490
37. Bojarskaite L, Nafari S, Ravnanger AK, et al. Role of aquaporin-4 polarization in extracellular solute clearance. *Fluids Barriers CNS*. 2024;21(1):28. doi: 10.1186/s12987-024-00527-7
38. Henneberger C, Bard L, Panatier A, et al. LTP induction boosts glutamate spillover by driving withdrawal of perisynaptic astroglia. *Neuron*. 2020;108(5):919-936.e11. doi: 10.1016/j.neuron.2020.08.030
39. Dossi E, Vasile F, Rouach N. Human astrocytes in the diseased brain. *Brain Res Bull*. 2017;136:139-156. doi: 10.1016/j.brainresbull.2017.02.001
40. Ortinski PI, Dong J, Mungenast A, et al. Selective induction of astrocytic gliosis generates deficits in neuronal inhibition. *Nat Neurosci*. 2010;13(5):584-591. doi: 10.1038/nn.2535
41. Robel S, Buckingham SC, Boni JL, et al. Reactive astrogliosis causes the development of spontaneous seizures. *J Neurosci*. 2015;35(8):3330-3345. doi: 10.1523/JNEUROSCI.1574-14.2015
42. Heffernan KS, Martinez I, Jaeger D, et al. Scaled complexity of mammalian astrocytes: insights from mouse and macaque. *J Comp Neurol*. 2024;532(8):e25665. doi: 10.1002/cne.25665
43. Ammothumkandy A, Ravina K, Wolseley V, et al. Altered adult neurogenesis and gliogenesis in patients with mesial temporal lobe epilepsy. *Nat Neurosci*. 2022;25(4):493-503. doi: 10.1038/s41593-022-01044-2
44. Corbin JG, Gaiano N, Juliano SL, Poluch S, Stancik E, Haydar TF. Regulation of neural progenitor cell development in the nervous system. *J Neurochem*. 2008;106(6):2272-2287. doi: 10.1111/j.1471-4159.2008.05522.x
45. Berg DA, Bond AM, Ming G li, Song H. Radial glial cells in the adult dentate gyrus: what are they and where do they come from? *F1000Research*. 2018;7:277. doi: 10.12688/f1000research.12684.1
46. Miranda-Negrón Y, García-Arrarás JE. Radial glia and radial glia-like cells: Their role in neurogenesis and regeneration. *Front Neurosci*. 2022;16. doi: 10.3389/fnins.2022.1006037
47. Encinas JM, Michurina TV, Peunova N, et al. Division-coupled astrocytic differentiation and age-related depletion of neural stem cells in the adult hippocampus. *Cell Stem Cell*. 2011;8(5):566-579. doi: 10.1016/j.stem. 2011.03.010